



Chinese Pharmaceutical Association
Institute of Materia Medica, Chinese Academy of Medical Sciences

Acta Pharmaceutica Sinica B

www.elsevier.com/locate/apsb
www.sciencedirect.com



ORIGINAL ARTICLE

Gastrin attenuates sepsis-induced myocardial dysfunction by down-regulation of TLR4 expression in macrophages



Dandong Fang^{a,b,g,†}, Yu Li^{a,b,†}, Bo He^{a,b,†}, Daqian Gu^{a,b,†},
Mingming Zhang^{a,b}, Jingwen Guo^{a,b}, Hongmei Ren^{a,b}, Xinyue Li^{a,b},
Ziyue Zhang^{a,b}, Ming Tang^{a,b}, Xingbing Li^{a,b}, Donghai Yang^{a,b},
Chunmei Xu^{a,b}, Yijie Hu^e, Hongyong Wang^{a,b}, Pedro A. Jose^f,
Yu Han^{a,b,*}, Chunyu Zeng^{a,b,c,d,*}

^aDepartment of Cardiology, Daping Hospital, the Third Military Medical University (Army Medical University), Chongqing 400000, China

^bKey Laboratory of Geriatric Cardiovascular and Cerebrovascular Disease Research, Ministry of Education of China, Chongqing Key Laboratory for Hypertension Research, Chongqing Cardiovascular Clinical Research Center, Chongqing Institute of Cardiology, Chongqing 400010, China

^cState Key Laboratory of Trauma, Burns and Combined Injury, Daping Hospital, the Third Military Medical University, Chongqing 400010, China

^dCardiovascular Research Center of Chongqing College, Chinese Academy of Sciences, University of Chinese Academy of Sciences Chongqing 400010, China

^eDepartment of Cardiac Surgery, Daping Hospital, Third Military Medical University, Chongqing 400010, China

^fDivision of Renal Disease & Hypertension, the George Washington University School of Medicine & Health Sciences, Washington, DC 20237, USA

^gDepartment of Critical Care Medicine, Jinling Hospital, Affiliated Hospital of Medical School, Nanjing University, Nanjing 210000, China

Received 12 December 2022; received in revised form 10 April 2023; accepted 6 June 2023

*Corresponding authors.

E-mail addresses: chunyuzeng01@163.com (Chunyu Zeng), hanc2-823@126.com (Yu Han).

[†]These authors made equal contributions to this work.

Peer review under the responsibility of Chinese Pharmaceutical Association and Institute of Materia Medica, Chinese Academy of Medical Sciences.

<https://doi.org/10.1016/j.apsb.2023.06.012>

2211-3835 © 2023 Chinese Pharmaceutical Association and Institute of Materia Medica, Chinese Academy of Medical Sciences. Production and hosting by Elsevier B.V. This is an open access article under the CC BY-NC-ND license (<http://creativecommons.org/licenses/by-nc-nd/4.0/>).

KEY WORDS

Sepsis-induced myocardial dysfunction;
 Gastrin;
 Cholecystokinin B receptor;
 Macrophage;
 Toll-like receptor 4;
 Peroxisome proliferators-activated receptor α ;
 Lipopolysaccharide;
 Inflammation

Abstract Myocardial dysfunction is the most serious complication of sepsis. Sepsis-induced myocardial dysfunction (SMD) is often associated with gastrointestinal dysfunction, but its pathophysiological significance remains unclear. The present study found that patients with SMD had higher plasma gastrin concentrations than those without SMD. In mice, knockdown of the gastrin receptor, cholecystokinin B receptor (*Cckbr*), aggravated lipopolysaccharide (LPS)-induced cardiac dysfunction and increased inflammation in the heart, whereas the intravenous administration of gastrin ameliorated SMD and cardiac injury. Macrophage infiltration plays a significant role in SMD because depletion of macrophages by the intravenous injection of clodronate liposomes, 48 h prior to LPS administration, alleviated LPS-induced cardiac injury in *Cckbr*-deficient mice. The intravenous injection of bone marrow macrophages (BMMs) overexpressing *Cckbr* reduced LPS-induced myocardial dysfunction. Furthermore, gastrin treatment inhibited toll-like receptor 4 (*TLR4*) expression through the peroxisome proliferator-activated receptor α (PPAR- α) signaling pathway in BMMs. Thus, our findings provide insights into the mechanism of the protective role of gastrin/CCKBR in SMD, which could be used to develop new treatment modalities for SMD.

© 2023 Chinese Pharmaceutical Association and Institute of Materia Medica, Chinese Academy of Medical Sciences. Production and hosting by Elsevier B.V. This is an open access article under the CC BY-NC-ND license (<http://creativecommons.org/licenses/by-nc-nd/4.0/>).

1. Introduction

Sepsis causes life-threatening multiple organ dysfunction due to a dysregulated host response to infection, and the in-hospital mortality rate of patients with septic shock is nearly 40%¹. Sepsis-induced myocardial dysfunction (SMD) is an important contributor to organ dysfunction in sepsis and has been reported in half of the patients with septic shock^{2,3}. Furthermore, septic patients with SMD have a mortality rate of 70%–90%, compared with 20% in septic patients without impairment of their cardiovascular system.⁴ Therefore, it is important to develop novel therapeutic approaches for SMD.

Gastrointestinal tract motility disorders are common complications of sepsis and can predict mortality^{5,6}. Patients with severe sepsis given enteral nutrition experience more severe sepsis and greater mortality than those receiving parenteral nutrition⁷. However, in critically ill patients without severe sepsis or septic shock, enteral nutrition is associated with fewer episodes of severe sepsis or septic shock than parenteral nutrition⁸. Enteral nutrition has beneficial effects in addition to delivering nutrients, such as maintenance of the gastrointestinal barrier and immunological and absorptive functions⁹. Enteral nutrition, relative to parenteral nutrition, is more effective in preserving gastrin secretion and motility of the gastrointestinal tract, decreasing inflammatory mediators, and maintaining the gastrointestinal mucosal barrier^{10,11}. The natriuresis following the ingestion of a specific amount of sodium may be due to the enterokine, gastrin, secreted by G cells in the stomach and duodenum and released into the circulation¹². Therefore, we investigated whether gastrin has a beneficial effect on cardiac function in patients with SMD. In the present study, we developed a rodent model of SMD by the intraperitoneal injection of lipopolysaccharide (LPS) into mice lacking the gastrin receptor, aka cholecystokinin B receptor (*Cckbr*). We found that the intravenous injection of gastrin, ameliorated SMD and cardiac injury by downregulating Toll-like receptor 4 (*Tlr4*) expression through the peroxisome proliferator-activated receptor α (PPAR- α) signaling pathway.

2. Methods**2.1. Study population**

Venous blood samples were collected in the morning on an empty stomach during the first 18 h after the diagnosis of sepsis in patients admitted to the intensive care unit ($n = 10$). Sepsis was defined according to the 2012 Surviving Sepsis Campaign guidelines¹³. Patients with sepsis and left ventricular ejection fraction (LVEF) <50%, cardiac troponin I >0.02 ng/mL, and B-type natriuretic peptide >300 pg/mL^{2,14} were selected for the current study. Age- and sex-matched healthy participants were used as controls ($n = 10$). Information on the controls and patients is listed in Table 1 (Army Medical Center of PLA #2022 No. 24). We have obtained written consent for each sample. The Acute Physiology and Chronic Health Evaluation (APACHE) II score system included 12 physiological variables (temperature, mean arterial pressure, heart rate, respiratory rate, A-a PO₂ (FiO₂ > 50%) or PaO₂ (FiO₂ < 50%), arterial pH or HCO₃⁻, serum sodium, potassium, creatinine, haematocrit, white blood cell count, and Glasgow Coma Scale), a chronic health evaluation, and an age adjustment score. Each variable

Table 1 Information on controls and patients.

Information (unit)	Control ($n = 10$)	Patient ($n = 10$)
Age (years)	57.3 ± 11.4	63.2 ± 14.7
Sex	4 F, 6 M	4 F, 6 M
EF (%)	62.5 ± 5.7	42.5 ± 4.7
cTnI (ng/mL)	0.010 ± 0.004	28.4 ± 12.6
BNP (pg/mL)	61.9 ± 19.2	467.3 ± 84.9
IL-1 β (pg/mL)	10.3 ± 3.8	136.2 ± 24.5
TNF- α (pg/mL)	11.7 ± 4.5	63.9 ± 16.9
IL-6 (pg/mL)	39.8 ± 16.4	167.4 ± 34.1
Procalcitonin (ng/mL)	ND	49.3 ± 28.8
APACHE II	NA	27.2 ± 9.1

F, female; M, male; NA, not applicable; ND, not determined.

was weighted from 0 to 4, and the total APACHE II score ranged from 0 to 71 points.¹⁵

2.2. Animals and SMD model

Cckbr-deficient (*Cckbr*^{-/-}) 129S2/SvPas mice were obtained from Jackson Laboratory¹⁶ and bred in the specific pathogen-free facility of the Third Military Medical University. Wild type (WT) 129S2/SvPas mice housed in the same cages were used as controls. The animals were housed in a controlled environment (20 ± 2 °C, 12 h/12 h light/dark cycles) with free access to water and standard rodent chow. We established the SMD model by the intraperitoneal injection of 200 µL LPS (25 mg/kg, *Escherichia coli*, Sigma–Aldrich, Burlington, USA)¹⁷. LPS was dissolved in phosphate-buffered saline (PBS) and saline was used as a control. Gastrin I (120 µg/kg, G1276, Sigma–Aldrich)¹⁸, dissolved in PBS, was injected into the tail vein. PBS without gastrin was used as a control. Echocardiography was performed to assess cardiac function in the mice 24 h after LPS injection. Thereafter, plasma was collected, and the mice were euthanised with 1% sodium pentobarbital (30 mg/kg, i.p.). The hearts and lungs were cleared off blood with pre-chilled PBS and frozen at -80 °C. The survival rate was observed for at least 60 h after the LPS injection. All experimental procedures were approved by the Animal Care and Use Committee of Third Military Medical University. All experiments conformed to the guidelines for the ethical use of animals, and efforts were made to minimise animal suffering and reduce the number of animals used.

2.3. Cardiac function

After induction of anaesthesia with inhalation of 2% isoflurane, the chest hair was removed with a depilatory agent, and then the mice were taped to a heated imaging platform. Echocardiography was performed using the Vevo 3100 imaging system equipped with a high-frequency transducer, based on the American Society of Echocardiography standard view. All images were analysed by a registered cardiovascular sonographer specialising in animal sonography, using the VisualSonics software package. To minimise bias, the studies were randomly presented to the measuring sonographers and date/time stamps were masked. All measurements were repeated thrice in three consecutive cardiac cycles and are reported as mean values. LVEF and left ventricular fractional shortening (LVFS) were measured using the M-mode.

2.4. Histological analysis

The hearts and lungs of mice were fixed in 4% paraformaldehyde for 48 h and dehydrated in increasing concentrations of ethanol. The treated hearts and lungs were cleared in xylene and embedded in paraffin. Slices were sectioned (4 µm), mounted on slides, deparaffinized, and rehydrated using successive incubation in xylene, 100% ethanol, 95% ethanol, 75% ethanol, and PBS. Pathological scoring was performed as previously described on a 0–4 scale¹⁹, in which 4 = diffuse inflammation with necrosis; 3 = diffuse mononuclear inflammation involving over 20% of the area, without necrosis; 2 = more than five distinct mononuclear inflammatory foci, or involvement of over 5% but not over 20% of the cross-sectional area; 1 = one to five distinct mononuclear inflammatory foci with involvement of 5% or less of the cross-sectional area; and 0 = no inflammation. Quantification was

conducted by an investigator blinded to the group information of the samples.

2.5. Terminal deoxynucleotidyl transferase dUTP nick-end labelling (TUNEL) assay

Apoptosis was detected using the TUNEL assay (Roche, Basel, Switzerland). In brief, the heart sections, placed on slides, were heated at 65 °C, washed in xylene, and dehydrated through a graded series of ethanol solutions. The sections were rinsed with PBS (5 min, thrice) and then incubated in 50 µL of TUNEL reaction mixture for 60 min at 37 °C in a humidified atmosphere in the absence of light. After washing with PBS (5 min, thrice), the sections were stained with 4',6-diamidino-2-phenylindole (DAPI). Images were captured using a fluorescence microscope (Eclipse Ti-U; Nikon Corporation, Tokyo, Japan) at an excitation wavelength of 405 nm for DAPI and 488 nm for TUNEL staining. The number of TUNEL-positive nuclei was quantified in 10 high-power fields from three different sections. The data are expressed as the average number of TUNEL-positive nuclei per high-power field. Quantification was conducted by an investigator blinded to the group information of the samples.

2.6. Biochemical assays

Blood from the patients and mice was collected into syringes containing sodium citrate (0.38% final concentration) to collect plasma. The blood samples were centrifuged at 4000 × *g* for 10 min for collection of plasma and then the plasma samples were stored at -80 °C. Enzyme-linked immunosorbent assay kits (Sangon Biotech, Shanghai, China) were used to measure the plasma concentrations of gastrin, cardiac troponin T (cTnT), and cardiac troponin I kits were used to measure serum creatinine and blood urea nitrogen (BUN) levels (Solarbio, Beijing, China). Serum alanine aminotransferase (ALT) and aspartate aminotransferase (AST) levels were quantified using a standard clinical automatic analyser with ALT or AST kits (Sigma–Aldrich).

2.7. Cell culture and transfection

The bone marrow macrophages (BMMs) were isolated using a standard protocol^{20,21}. BMMs were differentiated in Roswell Park Memorial Institute 1640 medium supplemented with 10% heat-inactivated foetal bovine serum that contained 20 ng/mL granulocyte-macrophage colony-stimulating factor (GM-CSF, Sino Biological Inc., Beijing, China) at 37 °C with 5% CO₂ in humidified air (Day 0). The entire culture medium was discarded on Day 3 and replaced with fresh, warmed medium containing GM-CSF (20 ng/mL). On Day 7, BMMs were used for subsequent experiments. For the anti-inflammatory experiments, BMMs were treated with LPS (100 ng/mL) and/or gastrin (10⁻⁷ mol/L)²² for 24 h. The vehicle groups were treated with the same volume (200 µL) of saline instead of drugs. *Ppar-α* was silenced using PPAR-specific shRNA infected with lentiviral particles (lenti-shPPAR-α, Santa Cruz Biotechnology, USA) on Day 4. Scramble shRNA infected with lentiviral particles (Santa Cruz Biotechnology) was used as the control. In these *in vitro* experiments, the cells were collected 3 days after infection to determine the efficiency of gene knockdown using qRT-PCR. A TLR4 inhibitor, TAK-242 (100 nmol/L, Resatorvid, MCE), was dissolved in *N,N*-dimethylformamide, diluted with the appropriate medium, and added to the cells directly before the addition of LPS (100 ng/mL).

To overexpress *Ppar- α* in BMMs, the cells were transfected with plasmids, 2 μ g empty vector, or 2 μ g pEnCMV-PPAR- α (Miaolingbio, Wuhan, China), according to the manufacturer's instructions.

2.8. Immunofluorescence microscopy

The heart sections on the glass slides were de-paraffinized and rehydrated. Antigens were retrieved by microwave, heating the heart sections in sodium citrate–EDTA antigen retrieval solution. The cells were fixed on glass slides and treated with 4% paraformaldehyde. After rinsing with PBS (5 min, thrice), the heart sections and cells were mixed with immunostaining blocking solution for 1 h at 25 °C to prevent nonspecific antibody binding. The heart sections and cells were then incubated with the primary antibody at 4 °C overnight. After washing with PBS (5 min, thrice), the heart sections and cells were incubated with the secondary antibody at room temperature for 1 h. Finally, after washing with PBS (5 min, thrice), the heart sections and cells were stained with DAPI before being imaged using a laser confocal scanning microscope. The following antibodies were used: F4/80 (Santa Cruz Biotechnology), P65 (Cell Signaling Technology), CCKBR (GeneTex, TX), FITC goat anti-mouse IgG (Proteintech, Wuhan, China), Cy3-conjugated goat anti-mouse IgG (Beyotime, Shanghai, China), Alexa Fluor™ Plus 647 donkey anti-goat IgG (Invitrogen, Carlsbad), and Cy3-conjugated donkey anti-goat IgG (Beyotime). Images were captured using a fluorescence microscope (Eclipse Ti-U). The images were collected by an investigator who was blinded to the group information of the samples.

2.9. Immunoblotting

The cytoplasmic and nuclear fractions were obtained using a Nuclear and Cytoplasmic Protein Extraction Kit (Beyotime, Shanghai, China). The protein samples were collected and stored at –20 °C until use. The protein samples were separated using sodium dodecyl-sulphate polyacrylamide gel electrophoresis on a 10%–15% polyacrylamide gel and then electroblotted onto nitrocellulose membranes (Amersham Life Science, Arlington). The blots were blocked in Tris-buffered saline containing 5% non-fat dry milk for 1 h at room temperature with constant shaking and then incubated with primary antibodies (P65, CCKBR, GAPDH, and histone H3) overnight at 4 °C. The secondary antibodies (goat anti-rabbit IR dye 800, donkey anti-goat IR dye 800, and goat anti-mouse IR dye 800) were used to bind the respective primary antibodies at room temperature for 1 h. The bound complexes were detected using an Odyssey Infrared Imaging System (Li-Cor Biosciences, Lincoln). The images were analysed using the Odyssey application software to obtain the integrated intensities. Information on these antibodies is provided in Supporting Information Table S1. The original images are shown in Supporting Information Fig. S9.

2.10. qRT-PCR

The cells were treated with saline vehicle, LPS (100 ng/mL), and/or gastrin (10^{-7} mol/L) for 24 h. Total RNA from tissues and cells was isolated using the Trizol procedure (Invitrogen). Two micrograms of total RNA were used to synthesize cDNA, which served as the template for the amplification of the different genes. The primers used to measure gene expression are listed in

Supporting Information Table S2. The amplification was performed under the following conditions: 94 °C for 2 min followed by 35 cycles of denaturation at 94 °C for 30 s, annealing at 58 °C for 30 s, and extension at 72 °C for 45 s. This was followed by a final extension at 72 °C for 10 min.

2.11. Macrophage depletion and adoptive transfer of macrophages

Clodronate liposomes (CLS), 200 μ L/mouse (Liposoma BV, Amsterdam, Netherlands) were intravenously injected 48 h before LPS administration to deplete macrophages in mice^{23,24}. The efficiency of depletion was confirmed using immunofluorescence analysis of the macrophages in the heart.

To overexpress *Cckbr* in BMMs, the cells were transfected with plasmids, 2 μ g empty vector, or 2 μ g pEnCMV-CCKBR (Miaolingbio), according to the manufacturer's instructions. The transfection mixture was removed 6 h post-transfection and complete medium containing 10% heat-inactivated foetal bovine serum was added. Subsequent experiments were performed 1 day after transfection. BMMs were transferred into mice, according to a published method²⁵. Briefly, 129S2/SvPas mice were intravenously injected with CLS to eliminate the macrophages. Then, after 24 h of the CLS injection, *Cckbr*-overexpressing BMMs (1×10^6 , 200 μ L) were intravenously injected into the mice. After 24 h, the mice were intraperitoneally injected with LPS (25 mg/kg, 200 μ L).

2.12. Statistical analysis

All data are expressed as the mean \pm standard deviation (SD), unless otherwise stated. GraphPad-Prism 8.0 and SPSS 17.0 were used to perform the statistical analysis. Student's unpaired *t*-test was used to compare two independent groups. In the experiments comparing multiple time points, separate *t*-tests were used for each time point. For comparison of ≥ 3 groups, analysis of variance was used with Tukey's *post hoc* test. Survival differences were assessed using Kaplan–Meier analysis followed by a log-rank test. All tests were two-tailed, and statistical significance was set at $P < 0.05$.

3. Results

3.1. Gastrin receptor deficiency aggravates LPS-induced myocardial dysfunction

To uncover the relationship between gastrin and SMD, we measured plasma gastrin concentration in ten SMD patients (two patients with cerebral infarction, three patients with cancer, and five patients with chronic obstructive pulmonary disease); ten healthy individuals were used as controls (Table 1). Plasma gastrin concentrations were more than double in patients with SMD compared with those in healthy controls (Fig. 1A). There was a positive correlation between plasma gastrin concentration and severity-of-disease APACHE II (Fig. 1B), indicating a possible role of gastrin in the pathogenesis of SMD.

To determine whether there is a causal relationship between gastrin and SMD, gastrin receptor-deficient (*Cckbr*^{–/–}) and WT mice were used to establish an SMD model through intraperitoneal injection of LPS (25 mg/kg, 200 μ L). Control mice with SMD had impaired cardiac function and increased plasma cTnT

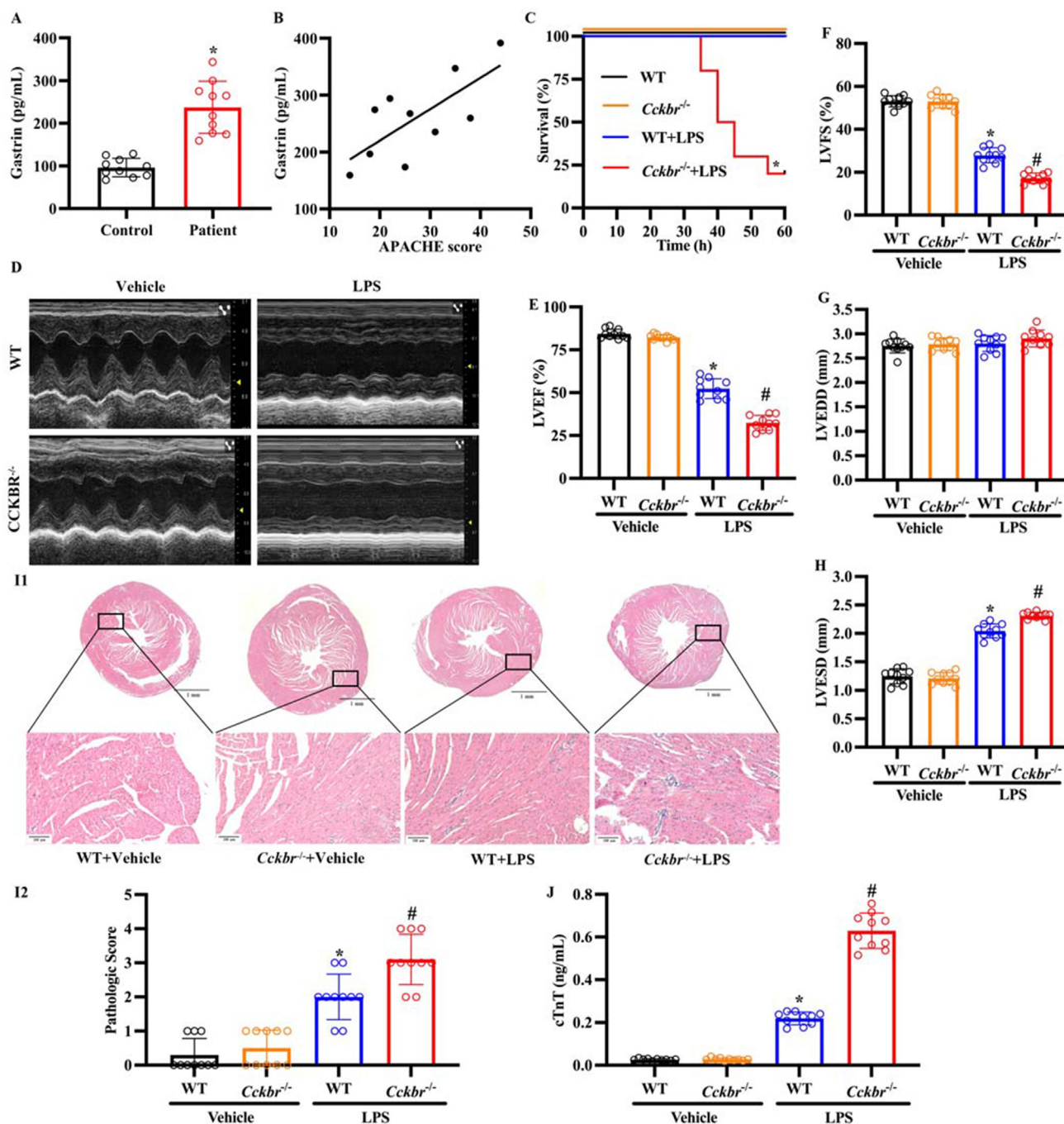


Figure 1 CCKBR deficiency aggravates LPS-induced cardiac dysfunction. (A) Plasma gastrin concentrations were measured using ELISA in patients with sepsis-induced myocardial dysfunction (SMD) and healthy controls ($n = 10$ per group). $*P < 0.05$ vs. control. (B) Correlation between plasma gastrin concentrations and APACHE (the Acute Physiology and Chronic Health Evaluation) II scores in SMD patients. Each dot represents a single patient. The solid line is the regression plot. (C) Kaplan–Meier (K–M) analysis for the different experimental groups: WT ($Cckbr^{+/+}$) mice, gastrin receptor knock-out ($Cckbr^{-/-}$) mice, WT mice with LPS treatment (25 mg/kg, 200 μ L, i.p., WT + LPS), $Cckbr^{-/-}$ mice with LPS treatment ($Cckbr^{-/-}$ + LPS). $n = 10$ per group; $*P < 0.05$ vs. WT + LPS treatment. (D–H) Echocardiography of WT ($Cckbr^{+/+}$) and $Cckbr^{-/-}$ mice with vehicle or LPS treatment (25 mg/kg, 200 μ L, i.p.). Representative M-mode images 24 h after LPS treatment (D) and quantitative analysis of the left ventricular (LV) EF (E) and FS (F), LVEDD (G), and LVESD (H). $n = 10$ per group; $*P < 0.05$ vs. WT + Vehicle; $\#P < 0.05$ vs. WT + LPS treatment. (I) Representative H&E staining images of heart tissues from the different groups (I1) and quantitative analysis of myocardial injury (I2). $n = 10$ per group; $*P < 0.05$ vs. WT + Vehicle; $\#P < 0.05$ vs. WT + LPS treatment. (J) cTnT levels were quantified using ELISA in WT ($Cckbr^{+/+}$) and $Cckbr^{-/-}$ mice with Vehicle or LPS treatment (25 mg/kg, i.p.). $n = 10$ per group; $*P < 0.05$ vs. WT + Vehicle; $\#P < 0.05$ vs. WT + LPS treatment.

concentration, and cardiac mRNA levels of *TNF- α* , *IL-1 β* , and *IL-6*, which are markers of inflammation (Supporting Information Fig. S1A–S1I). LPS treatment markedly increased the mortality of *Cckbr*^{-/-} mice (Fig. 1C). Cardiac function was assessed using echocardiography. LPS administration decreased LVEF and LVFS and increased left ventricular end-systolic diameter (LVESD) in WT mice. Although *Cckbr* deficiency had no effect on baseline cardiac function, it worsened cardiac function caused by LPS, shown by further decrease in LVEF and LVFS, and increase in LVESD (Fig. 1D–H). In addition, compared with WT mice, *Cckbr*^{-/-} mice exhibited higher cardiomyocyte apoptosis and cardiac inflammatory cell infiltration, and plasma cTnT concentration (Fig. 1I and J), accompanied with higher expression of markers of inflammation (*TNF- α* , *IL-1 β* , and *IL-6*) in the heart (Supporting Information Fig. S2A–S2D). Moreover, *Cckbr*^{-/-}

mice, compared with WT mice, had more severe injury to the lungs, kidneys, and liver after LPS treatment (Fig. S2E–S2I), indicating a protective role of CCKBR beyond cardiac function in the LPS-induced injury model.

3.2. Gastrin, through inhibition of macrophage infiltration in the heart, protects against LPS-induced myocardial dysfunction

To determine the mechanism of the protective role of gastrin on cardiac function, we injected gastrin (120 μ g/kg, 200 μ L) into the tail vein of mice immediately after the intraperitoneal injection of LPS (25 mg/kg, 200 μ L). Gastrin had no effect on cardiac function in vehicle-treated (control) mice (Fig. 2A–E), but ameliorated LPS-mediated cardiac impairment, as measured by LVEF, LVFS, and LVESD, but not left ventricular end-diastolic diameter

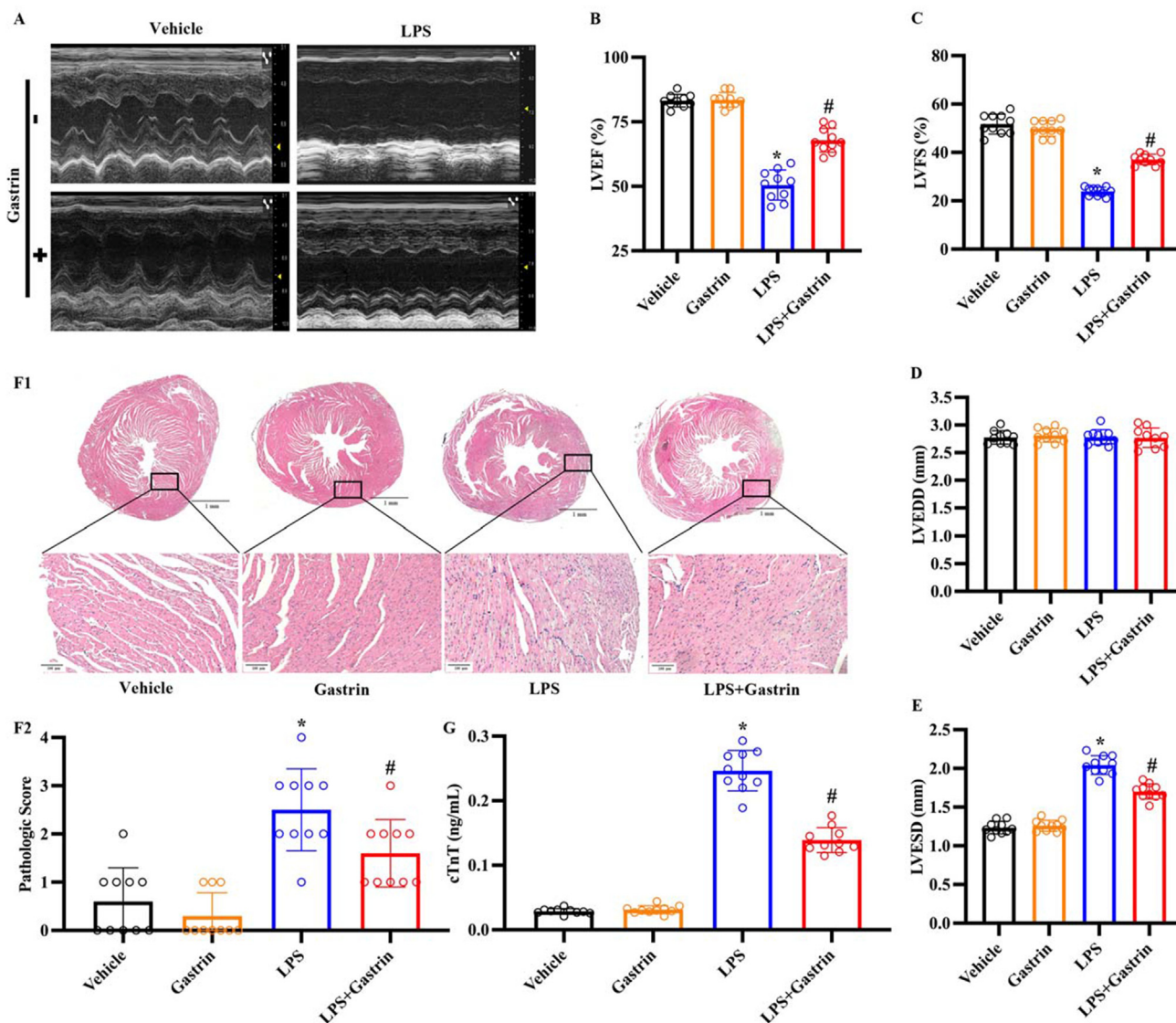


Figure 2 Gastrin attenuates LPS-induced cardiac dysfunction. (A–E) Echocardiography of 129S2/SvPas mice treated with Vehicle or LPS (25 mg/kg, i.p.), followed with gastrin treatment. Gastrin (120 μ g/kg) was injected into the tail vein immediately after LPS treatment. Representative M-mode images 24 h after treatment (A) and quantification of EF (B), FS (C), LVESD (E), and LVEDD (D). $n = 10$ per group; * $P < 0.05$ vs. vehicle; # $P < 0.05$ vs. LPS. (F) Representative images of H&E staining (F1) and quantitative analysis (F2) of myocardial injury. $n = 10$; * $P < 0.05$ vs. Vehicle treatment; # $P < 0.05$ vs. LPS treatment. (G) Plasma cTnT levels were quantified in 129S2/SvPas mice treated with vehicle alone or gastrin alone or also treated with LPS, as in (A). $n = 10$ per group; * $P < 0.05$ vs. Vehicle; # $P < 0.05$ vs. LPS.

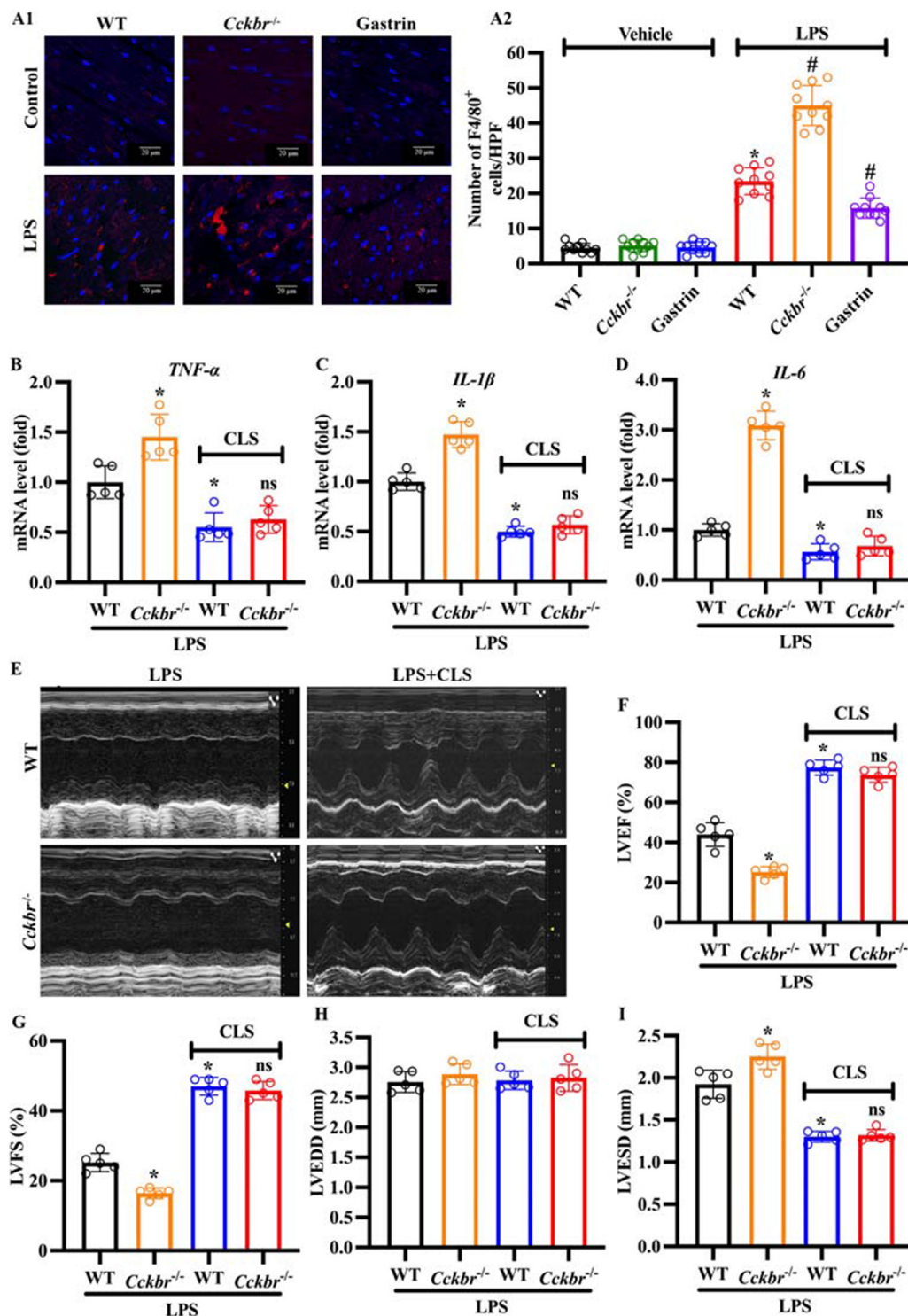


Figure 3 Gastrin/CCKBR ameliorates LPS-induced cardiac dysfunction by decreasing macrophage infiltration. (A) Represented images of F4/80 (macrophage marker, red) in the heart (A1) and quantification (A2) of F4/80⁺ staining cells per high power field (HPF). $n = 10$ per group; $*P < 0.05$ vs. WT + Vehicle; $^{\#}P < 0.05$ vs. WT + LPS treatment. (B–D) TNF- α , IL-1 β , and IL-6 mRNA expression in the heart of CCKBR wild type (WT) and *Cckbr*^{-/-} mice treated with CLS or vehicle (200 μ L, i.v.) 2 days before LPS injection (25 mg/kg, 200 μ L, i.p.). $n = 5$ per group; $*P < 0.05$ vs. WT + LPS treatment; $^{\text{ns}}P > 0.05$ vs. WT + LPS + CLS treatment. (E–I) Echocardiography of CCKBR wild type (WT) and *Cckbr*^{-/-} mice treated with vehicle or LPS. LPS and CLS treatments were the same as that in (B). Representative M-mode images and quantification of EF (F), FS (G), LVEDD (H), and LVESD (I). $n = 5$ per group; $*P < 0.05$ vs. WT + LPS treatment; $^{\text{ns}}P > 0.05$ vs. WT + LPS + CLS treatment.

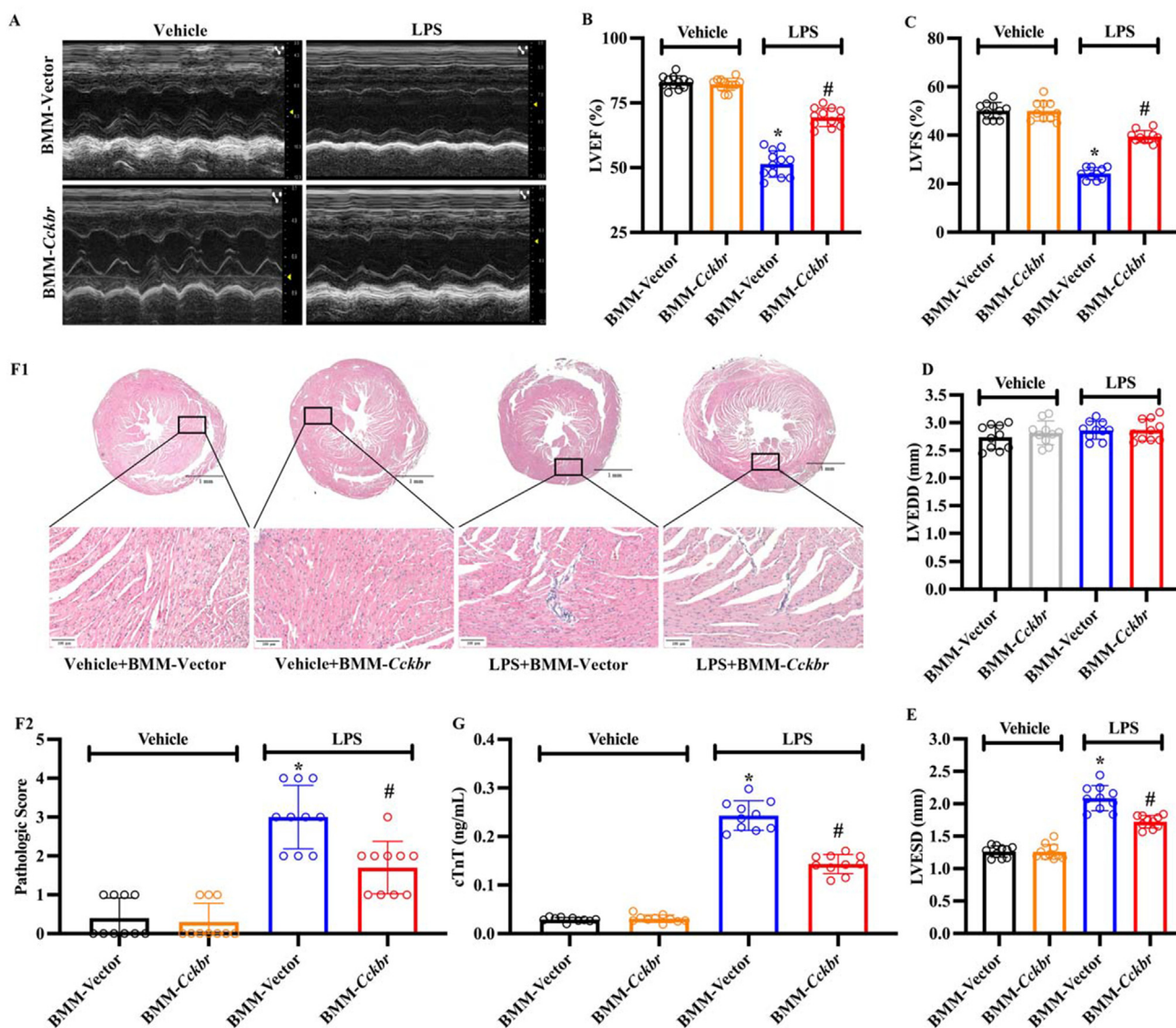


Figure 4 Adoptive transfer of CCKBR-overexpressed BMMs ameliorates LPS-induced cardiac dysfunction. (A–E) Echocardiography of 129S2/SvPas mice without (BMM-Vector) or with CCKBR-overexpressed BMMs (BMM-CCKBR) treated with vehicle or LPS (25 mg/kg, i.p.). Representative M-mode images (A) and quantification of EF (B), FS (C), LVEDD (D), and LVESD (E). $n = 10$ per group; * $P < 0.05$ vs. Vehicle + BMM-Vector; # $P < 0.05$ vs. LPS + BMM-Vector. (F) Representative images of H&E staining (F1) and quantitative analysis (F2) of myocardial injury in 129S2/SvPas mice without (BMM-Vector) or with CCKBR-overexpressed BMMs (BMM-CCKBR) and Vehicle or LPS treatment. $n = 10$ per group; * $P < 0.05$ vs. vehicle + BMM-Vector; # $P < 0.05$ vs. LPS + BMM-Vector. (G) Plasma cTnT levels in 129S2/SvPas mice with or without CCKBR-overexpressed BMMs and LPS treatment. $n = 10$ per group; * $P < 0.05$ vs. Vehicle + BMM-Vector treatment; # $P < 0.05$ vs. LPS + BMM-vector treatment.

(LVEDD) (Fig. 2A–E) and decreased inflammatory cell infiltration of the heart, cardiomyocyte apoptosis, and plasma cTnT (Fig. 2F and G and Supporting Information Fig. S3A), accompanied by decreased levels of inflammation-related genes (*TNF- α* , *IL-1 β* , and *IL-6*) in the heart (Fig. S3B–S3D). Moreover, the protective effect of gastrin in LPS-treated mice was observed throughout the body, as shown by the protection against LPS-induced lung injury (Fig. S3E) and mitigation of the increase in BUN and serum creatinine, ALT, and AST levels in mice with SMD (Fig. S3F–S3I).

Because macrophages are important in the pathogenesis of SMD²⁶, we studied macrophage infiltration in the heart 24 h after

LPS treatment. *Cckbr* deficiency increased, whereas gastrin treatment decreased the macrophage infiltration in the heart (Fig. 3A). The depletion of macrophages by the intravenous injection of CLS 48 h prior to LPS administration (Supporting Information Fig. S4) reduced LPS-induced inflammation in the heart (Fig. 3B–D), and simultaneously alleviated the cardiac dysfunction (measured by LVEF, LVFS, and LVESD) to the same extent in WT and *Cckbr*^{-/-} mice (Fig. 3E–I). *In vitro*, gastrin also mitigated the LPS-induced upregulation of *TNF- α* , *IL-1 β* , and *IL-6* in BMMs (Supporting Information Fig. S5A–S5C), indicating that gastrin and its receptor, through inhibition of macrophage infiltration into the heart, protect against SMD.

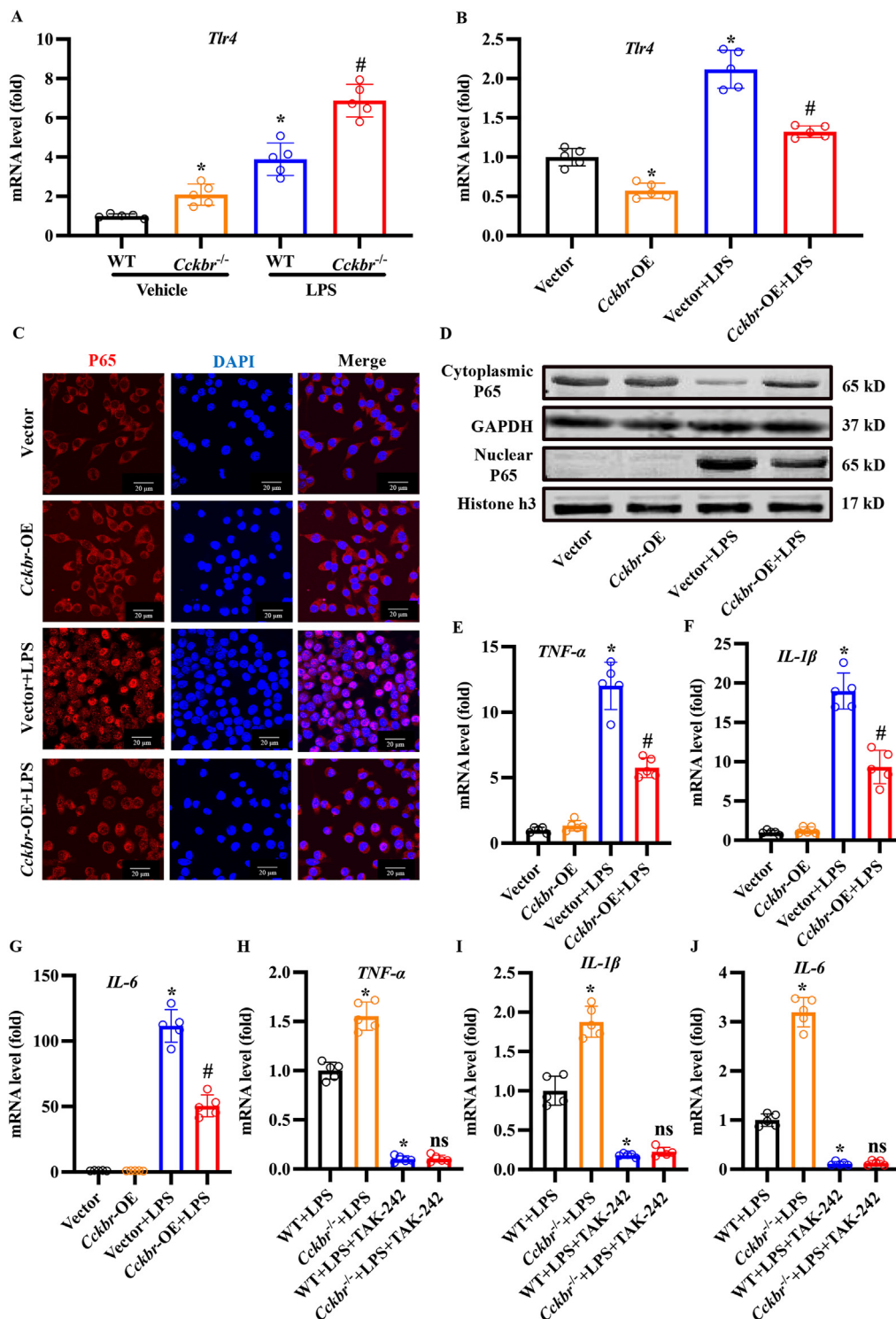


Figure 5 CCKBR inhibits the expression of TLR4 and its downstream activation in BMMs. (A) TLR4 mRNA expression in BMMs from *Cckbr*^{-/-} or WT mice treated with Vehicle or LPS (100 ng/mL) for 24 h $n = 5$ per group; * $P < 0.05$ vs. WT + Vehicle, # $P < 0.05$ vs. WT + LPS. (B) TLR4 mRNA expression in BMMs from 129S2/SvPas mice. BMMs treated with vehicle or LPS (100 ng/mL) for 24 h after CCKBR overexpression (CCKBR-OE) by transfection with pEnCMV-CCKBR. $n = 5$ per group; * $P < 0.05$ vs. vector; # $P < 0.05$ vs. Vector + LPS treatment. (C) Represented immunofluorescence images with double staining of P65 (red) and DAPI (blue) in BMMs from 129S2/SvPas mice. The BMMs not over expressing (Vector) or overexpressing CCKBR (CCKBR-OR) by transfection with pEnCMV-CCKBR were treated with Vehicle (no LPS) or LPS. (D) Western blots of cytoplasmic and nuclear P65 in BMMs from 129S2/SvPas mice. The BMMs were treated with Vehicle or LPS as in (B) and (C). $n = 5$ per group. (E–G) TNF- α , IL-1 β , and IL-6 mRNA expression in BMMs treated with LPS in BMMs not overexpressing CCKBR (Vector) or overexpressing CCKBR by transfection with pEnCMV-CCKBR (CCKBR-OE) as that in (B). TNF- α (E), IL-1 β (F), and IL-6 (G) levels. $n = 5$ per group; * $P < 0.05$ vs. Vector only; # $P < 0.05$ vs. Vector + LPS treatment. (H–J) Proinflammatory cytokines mRNA expression in BMMs from WT and *Cckbr*^{-/-} mice treated with LPS and TLR4 inhibitor TAK-242 (100 nmol/L): TNF- α (H), IL-1 β (I), and IL-6 (J) levels. $n = 5$ per group; * $P < 0.05$ vs. WT + LPS treatment; ns $P > 0.05$ vs. WT + LPS + TAK-242 treatment.

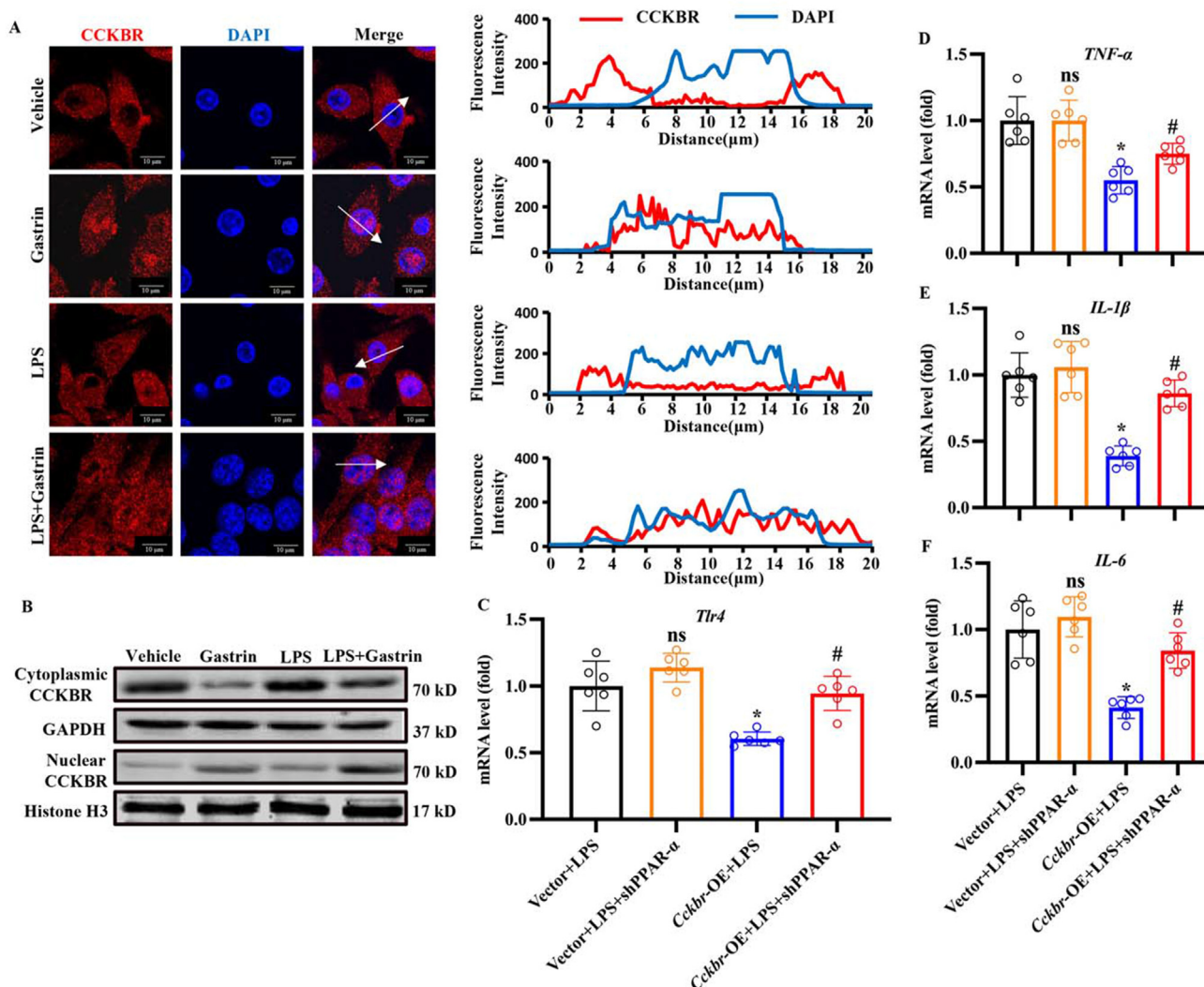


Figure 6 CCKBR/gastrin reduces LPS-induced inflammation in BMMs through PPAR- α . (A) Representative immunofluorescence images with double staining of CCKBR (red) and DAPI (blue) in BMMs treated with Vehicle, Gastrin (10^{-7} mol/L) alone, LPS (100 ng/mL) alone, or LPS + Gastrin for 24 h. The representative fluorescent images (left) and line intensity profiles (right) were acquired from the white arrows; the abscissa value is the distance from the detection point to the tail of the arrow. (B) Western blot analyses of nuclear and cytoplasmic distribution of CCKBR in BMMs treated with Vehicle, Gastrin (10^{-7} mol/L) alone, LPS (100 ng/mL) alone, or LPS + Gastrin for 24 h. (C) TLR4 mRNA expression in BMMs without CCKBR overexpression (Vector) or CCKBR overexpression (CCKBR-OE) with or without shPPAR- α and LPS treatment (100 ng/mL). $n = 6$ per group; $^{ns}P > 0.05$ Vector + LPS + shPPAR- α vs. Vector + LPS treatment; $*P < 0.05$ CCKBR-OE + LPS treatment vs. Vector + LPS treatment; $^{\#}P < 0.05$ vs. CCKBR-OE + LPS treatment. (D–F) Proinflammatory cytokines mRNA expressions in BMMs treated as that in (C). TNF- α (D), IL-1 β (E), and IL-6 (F) levels. $n = 6$; $^{ns}P > 0.05$ vs. Vector + LPS treatment; $*P < 0.05$ vs. Vector + LPS treatment; $^{\#}P < 0.05$ vs. CCKBR-OE + LPS treatment.

3.3. Transfer of *Cckbr*-overexpressed BMMs ameliorates LPS-induced myocardial dysfunction

Gastrin exerts its effects by acting on its receptor, CCKBR²⁷. Therefore, to determine further the role of gastrin and macrophages on the LPS-induced myocardial dysfunction, BMMs were over-expressed with *Cckbr* (BMM-*Cckbr*) and then used to treat mice with SMD. BMMs (1×10^6 , 200 μ L) transfected with pEnCMV-CCKBR were injected into the tail vein of mice the day after macrophage depletion using CLS²⁵. One day after the adaptive transfer, the mice were intraperitoneally injected with

vehicle (200 μ L) or LPS (25 mg/mL, 200 μ L). We found that BMM-*Cckbr* treatment reduced the LPS-induced impairment of cardiac function (LVEF, LVFS, and LVESD), as measured using echocardiography (Fig. 4A–E), accompanied by less inflammatory cell infiltration and cardiomyocyte apoptosis, and decreased plasma cTnT concentration (Fig. 4F and G and Supporting Information Fig. S6A). Moreover, the transfer of BMM-*Cckbr* mitigated inflammation, as shown by the decrease in TNF- α , IL-1 β , and IL-6 levels in the heart (Fig. S6B–S6D). The protective effect of BMM-*Cckbr* treatment was exerted throughout the body, proved by the mitigation of the increase in BUN and serum

creatinine, ALT, and AST levels in SMD mice (Fig. S6E–S6H). Therefore, our data demonstrate the importance of CCKBR in BMMs in ameliorating LPS-induced myocardial dysfunction.

3.4. Gastrin inhibits macrophage inflammation through inhibition of *Tlr4* expression

Toll-like receptor 4 (TLR4) initiates MyD88-dependent pathways which activate proinflammatory cytokines, such as NF- κ B P65^{28,29}. Consistent with other reports³⁰, our present study found that *Cckbr* knockout increased (Fig. 5A), whereas overexpression of *Cckbr* (*Cckbr*-OE) (Supporting Information Fig. S7A and S7B) decreased LPS-induced *Tlr4* expression in BMMs (Fig. 5B). In addition, *Cckbr*-OE reduced the translocation of NF- κ B P65 from the cytosol to the nucleus (Fig. 5C and D), accompanied by decreased expression of *TNF- α* , *IL-1 β* , and *IL-6* in BMMs (Fig. 5E–G). Moreover, the mild increase in LPS-treated BMMs from WT and marked increase in LPS-treated BMMs from *Cckbr*^{-/-} mice were blocked by TAK-242, a TLR4 inhibitor³¹ (Fig. 5H–J). These results indicate that CCKBR can downregulate TLR4/NF- κ B and suppress inflammation.

Our previous study found that gastrin can stimulate CCKBR to translocate from the cytosol to the nucleus and function as a transcription factor to increase *Ppar- α* expression³². Our present study shows that *Cckbr*-OE increased, while *Cckbr* knockout decreased *Ppar- α* expression in primary BMMs in the basal state, *i.e.*, vehicle-treatment (Supporting Information Fig. S8A). Moreover, we found that LPS inhibited *Ppar- α* expressions in primary BMMs from both WT and *Cckbr*^{-/-} mice, which was rescued by gastrin treatment or *Cckbr*-OE in BMMs from WT mice (Fig. S8A). The importance of PPAR- α on the CCKBR-mediated inhibitory effect on inflammation was supported by our finding that overexpression of *Ppar- α* in *Cckbr*^{-/-} BMMs could reverse the aggravating effect of *Cckbr* gene knockout on inflammatory factors (Fig. S8B–S8F).

PPAR- α can downregulate *Tlr4* expression and reduce inflammation^{33–36}. Therefore, we considered whether PPAR- α mediates the ability of CCKBR to decrease *Tlr4* expression. We found that gastrin increased CCKBR translocation from the cytosol to the nucleus in BMMs, as determined by immunofluorescence and Western blot analyses (Fig. 6A and B). Downregulation of *Ppar- α* expression by shRNA inhibited the ability of CCKBR to decrease *Tlr4* expression in LPS-treated BMMs (Fig. 6C). Moreover, the downregulation of *TNF- α* , *IL-1 β* , and *IL-6* with *Cckbr*-OE was inhibited by shPPAR- α (Fig. 6D–F), confirming that gastrin downregulates *Tlr4* expression by stimulating *Ppar- α* .

4. Discussion

Gastrointestinal hormones play an important role in the maintenance of cardiovascular homeostasis^{37–41}. Among these hormones, gastrin is a stress-related hormone produced by G cells with chemo-mechanical stimulation (neural, hormonal, luminal, mechanical, and inflammatory factors)^{42,43} and has cardioprotective effects in myocardial ischaemia-reperfusion injury and myocardial infarction.^{44,45} Sepsis is associated with the release of gut peptides, including gastrin^{46,47}; however, the role of increased gastrin levels in sepsis or SMD is unknown. The present study demonstrates that gastrin exerts a protective effect against sepsis-induced myocardial injury and, therefore, improves cardiac function.

Motility disorders of the gastrointestinal tract are common complications of sepsis^{5,6}. Randomised controlled studies that compared enteral and parenteral nutrition in patients admitted to the intensive care unit showed that patients who received enteral nutrition had fewer episodes of severe sepsis or septic shock⁸. Enteral nutrition also reduces sepsis-related mortality and morbidity in patients with major burn injury⁴⁸. Therefore, nutrition guidelines suggest early enteral nutrition in critically ill patients^{49,50}. However, the underlying mechanisms involved in the protective effect of enteral nutrition against sepsis are not completely understood. Recent studies have shown that enteral nutrition is crucial to maintain gastrointestinal functions, such as barrier, immunological, and absorptive functions⁹, and the secretion of gastrointestinal hormones is believed to play an important role in these processes^{9–11}. We wondered which hormone plays a critical role in the protection of cardiac function in SMD. Some studies have shown that sepsis increases gastrin secretion^{46,47}. Studies have also shown that plasma gastrin concentration decreases after parenteral nutrition^{10,11} but increases after enteral nutrition²². Therefore, in this study, we focused on gastrin. Our results showed that gastrin treatment ameliorated SMD and cardiac injury by downregulating *Tlr4* expression through the PPAR- α signaling pathway.

Macrophages play a crucial role in host defence against a variety of pathogens and the inflammatory immune response during sepsis⁵¹. Indeed, macrophage depletion increases the mortality caused by sepsis^{52,53}. Gastrin stimulates CCKBR in macrophages and enhances efferocytosis³², and macrophages play important roles in cardiac function and remodelling⁵⁴. Therefore, we investigated the role of gastrin/CCKBR in macrophage-mediated LPS-induced fulminant heart injuries. Depletion of macrophages using CLS mitigated endotoxin-induced cardiac injury in *Cckbr* deficient mice. Moreover, the transfer of BMM-*Cckbr* ameliorated endotoxin-induced myocardial dysfunction, demonstrating the importance of CCKBR in BMM-derived macrophages for the treatment of SMD. We found that BMM depletion with CLS prior to LPS treatment had a better protective effect than BMM-*Cckbr* transfer on LVEF, which might be explained by the differentiation of some BMMs into M1. It is known that M1 macrophage is harmful to cardiac function^{55,56}. However, we have to state that with LPS treatment the LVEF in the BMM-*Cckbr* group is better than that in the BMM control group, showing the beneficial effect of CCKBR in LPS-induced cardiac dysfunction. Nevertheless, we realize the limitations of the present study. The protective effects of gastrin/CCKBR on cardiac function are multiple. Our previous study found that gastrin protects cardiomyocytes against ischemia/reperfusion injury through activation of the RISK and SAFE pathways⁴². However, we have to indicate that the direct protection on cardiomyocyte is marginal, because after depletion of macrophages, the cardiac function, as measured by LVEF, was not different between WT and *Cckbr*^{-/-} mice treated with LPS. Therefore, the major mechanism of the beneficial effect of CCKBR on cardiac function relies on the presence of macrophages.

TLR4 is the main receptor for sensing LPS²⁸. TLR4 in leukocytes, as in macrophages, instead of that in cardiomyocytes, plays an essential role in the cardiac impairment during endotoxemia⁵⁷. Activated TLR4 stimulates NF- κ B signaling which increases the release of inflammatory cytokines²⁹. Our present study showed that gastrin treatment prevented LPS-induced *Tlr4* expression in BMMs, and consequently inhibited NF- κ B signaling and the release of inflammatory cytokines. CCKBR, as a transcription factor of *Ppar- α* , has been reported in our previous study²⁹, and the present study found that the inhibitory effect of

CCKBR on TLR4 occurs through the activation of *Ppar- α* . Consistent with the report of others^{58,59}, our present study showed that *Ppar- α* inactivation, by itself, had no effect on the LPS-mediated induction of inflammatory genes in WT BMM, which may be ascribed to the inability of BMMs to synthesize gastrin^{60,61}. Therefore, in BMMs in the basal state, without gastrin stimulation, the inactivation of *Ppar- α* , alone, has no effect on LPS-induced inflammatory gene expression.

The physiological function of gastrin is mainly to stimulate parietal cells to produce gastric acid⁶², which increases the occurrence of ulcers and bleeding in critically ill patients^{63,64}. Thus, gastrin treatment in SMD may increase the risk of developing gastric ulcers and the related side effects. Therefore, we changed our therapeutic strategy from gastrin treatment to CCKBR modification in BMMs. The present study showed that the intravenous injection of *Cckbr*-OE BMMs exerted a protective effect against LPS-induced cardiac function impairment.

In summary, gastrin/CCKBR plays a protective role against SMD by inhibiting *Tlr4* expression through the PPAR- α signaling pathway.

5. Conclusions

Gastrin/CCKBR was able to attenuate the severity of SMD. By inhibiting the expression of *Tlr4*, gastrin/CCKBR can impair the translocation of NF- κ B P65 from the cytosol to the nucleus, thereby inhibiting the expression of proinflammatory factors and attenuating the damage in the heart and other organs caused by LPS.

Acknowledgments

This study was supported by grants to Chunyu Zeng from the Program of Innovative Research Team by National Natural Science Foundation (81721001, China), National Natural Science Foundation of China (31430043, 31730043), Program for Changjiang Scholars, and Innovative Research Team in University (IRT1216, China); and the National Key R&D Program of China (2018YFC1312700); and by grant to Jingwen Guo from the National Natural Science Foundation of China (82000476); and by grant to Yijie Hu from the Excellent Talents Project of Third Military Medical University (B-3232, China); by grant to Hongyong Wang from the Clinical Technology Innovation and Cultivation Program of AMU (CX2019JS220, China); by grant to Xinyue Li from Chongqing Natural Science Foundation (CSTB2022NSCQ-BHX0025, China).

Author contributions

We declare that all authors made fundamental contributions to the manuscript. Chunyu Zeng, Dandong Fang and Yu Han designed the study. Dandong Fang, Yu Li, Bo He, Daqian Gu, Hongmei Ren, Ziyue Zhang and Chunmei Xu carried out experiments. Mingming Zhang, Jingwen Guo, Xinyue Li, Ming Tang, Xingbing Li, and Donghai Yang analyzed the data. Dandong Fang prepared the manuscript. Yijie Hu, Hongyong Wang and Pedro A. Jose advised the experiment. All authors revised the manuscript and approved the final version.

Conflicts of interest

The authors declare no conflicts of interest.

Appendix A. Supporting information

Supporting data to this article can be found online at <https://doi.org/10.1016/j.apsb.2023.06.012>.

References

- Singer M, Deutschman CS, Seymour CW, Shankar-Hari M, Annane D, Bauer M, et al. The Third international consensus definitions for sepsis and septic shock (Sepsis-3). *JAMA* 2016;**315**: 801–10.
- Beesley SJ, Weber G, Sarge T, Nikravan S, Grissom CK, Lanspa MJ, et al. Septic cardiomyopathy. *Crit Care Med* 2018;**46**:625–34.
- Landesberg G, Gilon D, Meroz Y, Georgieva M, Levin PD, Goodman S, et al. Diastolic dysfunction and mortality in severe sepsis and septic shock. *Eur Heart J* 2012;**33**:895–903.
- Merx MW, Weber C. Sepsis and the heart. *Circulation* 2007;**116**: 793–802.
- Bruins MJ, Luiking YC, Soeters PB, Akkermans LM, Deutz NE. Effect of prolonged hyperdynamic endotoxemia on jejunal motility in fasted and enterally fed pigs. *Ann Surg* 2003;**237**:44–51.
- Adike A, Quigley EM. Gastrointestinal motility problems in critical care: a clinical perspective. *J Dig Dis* 2014;**15**:335–44.
- Bertolini G, Iapichino G, Radrizzani D, Facchini R, Simini B, Bruzzone P, et al. Early enteral immunonutrition in patients with severe sepsis: results of an interim analysis of a randomized multicentre clinical trial. *Intensive Care Med* 2003;**29**:834–40.
- Radrizzani D, Bertolini G, Facchini R, Simini B, Bruzzone P, Zanforlin G, et al. Early enteral immunonutrition vs. parenteral nutrition in critically ill patients without severe sepsis: a randomized clinical trial. *Intensive Care Med* 2006;**32**:1191–8.
- Schorhuber M, Fruhwald S. Effects of enteral nutrition on gastrointestinal function in patients who are critically ill. *Lancet Gastroenterol Hepatol* 2018;**3**:281–7.
- Johnson LR, Copeland EM, Dudrick SJ, Lichtenberger LM, Castro GA. Structural and hormonal alterations in the gastrointestinal tract of parenterally fed rats. *Gastroenterology* 1975;**68**:1177–83.
- Chen Z, Wang S, Yu B, Li A. A comparison study between early enteral nutrition and parenteral nutrition in severe burn patients. *Burns* 2007;**33**:708–12.
- Jose PA, Yang Z, Zeng C, Felder RA. The importance of the gastrorenal axis in the control of body sodium homeostasis. *Exp Physiol* 2016;**101**:465–70.
- Dellinger RP, Levy MM, Rhodes A, Annane D, Gerlach H, Opal SM, et al. Surviving sepsis campaign: international guidelines for management of severe sepsis and septic shock, 2012. *Intensive Care Med* 2013;**39**:165–228.
- De Geer L, Engvall J, Oscarsson A. Strain echocardiography in septic shock—a comparison with systolic and diastolic function parameters, cardiac biomarkers and outcome. *Crit Care* 2015;**19**:122.
- Knaus WA, Draper EA, Wagner DP, Zimmerman JE. Apache II: a severity of disease classification system. *Crit Care Med* 1985;**13**: 818–29.
- Langhans N, Rindi G, Chiu M, Rehfeld JF, Ardman B, Beinborn M, et al. Abnormal gastric histology and decreased acid production in cholecystokinin-B/gastrin receptor-deficient mice. *Gastroenterology* 1997;**112**:280–6.
- Xu D, Yang F, Chen J, Zhu T, Wang F, Xiao Y, et al. Novel STING-targeted PET radiotracer for alert and therapeutic evaluation of acute lung injury. *Acta Pharm Sin B* 2023;**13**:2124–37.
- Fu J, Tang Y, Zhang Z, Tong L, Yue R, Cai L. Gastrin exerts a protective effect against myocardial infarction via promoting angiogenesis. *Mol Med* 2021;**27**:90.
- Li M, Wang X, Xie Y, Xie Y, Zhang X, Zou Y, et al. Initial weight and virus dose: two factors affecting the onset of acute coxsackievirus B3 myocarditis in C57BL/6 mouse—a histopathology-based study. *Cardiovasc Pathol* 2013;**22**:96–101.

20. Weischenfeldt J, Porse B. Bone marrow-derived macrophages (BMM): isolation and applications. *CSH Protoc* 2008;**2008**:pdb prot5080.
21. Ye J, Zeng B, Zhong M, Li H, Xu L, Shu J, et al. Scutellarin inhibits caspase-11 activation and pyroptosis in macrophages via regulating PKA signaling. *Acta Pharm Sin B* 2021;**11**:112–26.
22. Chen Y, Asico LD, Zheng S, Villar VA, He D, Zhou L, et al. Gastrin and D1 dopamine receptor interact to induce natriuresis and diuresis. *Hypertension* 2013;**62**:927–33.
23. Wernli G, Hasan W, Bhattacharjee A, van Rooijen N, Smith PG. Macrophage depletion suppresses sympathetic hyperinnervation following myocardial infarction. *Basic Res Cardiol* 2009;**104**:681–93.
24. Wu Y, Luo X, Zhou Q, Gong H, Gao H, Liu T, et al. The disbalance of LRP1 and SIRPalpha by psychological stress dampens the clearance of tumor cells by macrophages. *Acta Pharm Sin B* 2022;**12**:197–209.
25. Kong XN, Yan HX, Chen L, Dong LW, Yang W, Liu Q, et al. LPS-induced down-regulation of signal regulatory protein α contributes to innate immune activation in macrophages. *J Exp Med* 2007;**204**:2719–31.
26. Sun Z, Zhou D, Xie X, Wang S, Wang Z, Zhao W, et al. Cross-talk between macrophages and atrial myocytes in atrial fibrillation. *Basic Res Cardiol* 2016;**111**:63.
27. Lamers CB. The significance of gastrin in the pathogenesis and therapy of peptic ulcer disease. *Drugs* 1988;**35**(Suppl 3):10–6.
28. Lim KH, Staudt LM. Toll-like receptor signaling. *Cold Spring Harbor Perspect Biol* 2013;**5**:a011247.
29. Kondo T, Kawai T, Akira S. Dissecting negative regulation of Toll-like receptor signaling. *Trends Immunol* 2012;**33**:449–58.
30. Koks S, Fernandes C, Kurrikoff K, Vasar E, Schalkwyk LC. Gene expression profiling reveals upregulation of Tlr4 receptors in Cckb receptor deficient mice. *Behav Brain Res* 2008;**188**:62–70.
31. Li M, Matsunaga N, Hazeki K, Nakamura K, Takashima K, Seya T, et al. A novel cyclohexene derivative, ethyl (6R)-6-[N-(2-cFluoro-4-fluorophenyl)sulfamoyl]cyclohex-1-ene-1-carboxylate (TAK-242), selectively inhibits toll-like receptor 4-mediated cytokine production through suppression of intracellular signaling. *Mol Pharmacol* 2006;**69**:1288–95.
32. Gu D, Fang D, Zhang M, Guo J, Ren H, Li X, et al. Gastrin, via activation of PPAR α , protects the kidney against hypertensive injury. *Clin Sci Lond* 2021;**135**:409–27.
33. Esposito G, Capoccia E, Turco F, Palumbo I, Lu J, Steardo A, et al. Palmitoylethanolamide improves colon inflammation through an enteric glia/toll like receptor 4-dependent PPAR- α activation. *Gut* 2014;**63**:1300–12.
34. Dana N, Haghjooy Javanmard S, Vaseghi G. The effect of fenofibrate, a PPAR α activator on toll-like receptor-4 signal transduction in melanoma both *in vitro* and *in vivo*. *Clin Transl Oncol* 2020;**22**:486–94.
35. Han X, Chen D, Liufu N, Ji F, Zeng Q, Yao W, et al. MG53 protects against sepsis-induced myocardial dysfunction by upregulating peroxisome proliferator-activated receptor- α . *Oxid Med Cell Longev* 2020;**2020**:7413693.
36. Standage SW, Bennion BG, Knowles TO, Ledee DR, Portman MA, McGuire JK, et al. PPARalpha augments heart function and cardiac fatty acid oxidation in early experimental polymicrobial sepsis. *Am J Physiol Heart Circ Physiol* 2017;**312**:H239–49.
37. Sweeney G. Cardiovascular effects of leptin. *Nat Rev Cardiol* 2010;**7**:22–9.
38. Drucker DJ. The cardiovascular biology of glucagon-like peptide-1. *Cell Metabol* 2016;**24**:15–30.
39. Cao JM, Ong H, Chen C. Effects of ghrelin and synthetic GH secretagogues on the cardiovascular system. *Trends Endocrinol Metabol* 2006;**17**:13–8.
40. Grossini E, Caimmi P, Molinari C, Uberti F, Mary D, Vacca G. Intracoronary gastrin 17 increases cardiac perfusion and function through autonomic nervous system, CCK receptors, and nitric oxide in anesthetized pigs. *J Appl Physiol* 2011;**110**:95–108.
41. Pang J, Feng JN, Ling W, Jin T. The anti-inflammatory feature of glucagon-like peptide-1 and its based diabetes drugs—therapeutic potential exploration in lung injury. *Acta Pharm Sin B* 2022;**12**:4040–55.
42. Kidd M, Hauso O, Drozdov I, Gustafsson BI, Modlin IM. Delineation of the chemomechanosensory regulation of gastrin secretion using pure rodent G cells. *Gastroenterology* 2009;**137**:231–241.e10.
43. Weigert N, Schaffer K, Schusdziarra V, Classen M, Schepp W. Gastrin secretion from primary cultures of rabbit antral G cells: stimulation by inflammatory cytokines. *Gastroenterology* 1996;**110**:147–54.
44. Wang R, Zhang Z, Xu Z, Wang N, Yang D, Liu ZZ, et al. Gastrin mediates cardioprotection through angiogenesis after myocardial infarction by activating the HIF-1 α /VEGF signalling pathway. *Sci Rep* 2021;**11**:15836.
45. Yang X, Yue R, Zhang J, Zhang X, Liu Y, Chen C, et al. Gastrin protects against myocardial ischemia/reperfusion injury via activation of RISK (reperfusion injury salvage kinase) and SAFE (survivor activating factor enhancement) pathways. *J Am Heart Assoc* 2018;**7**:165–228.
46. Kim YS, Chang LK, Mercer DW. Lipopolysaccharide-induced gastroprotection is independent of the vagus nerve. *Dig Dis Sci* 2001;**46**:1526–32.
47. Zamir O, Hasselgren PO, Higashiguchi T, Frederick JA, Fischer JE. Effect of sepsis or cytokine administration on release of gut peptides. *Am J Surg* 1992;**163**:181–4 [discussion 4–5].
48. Pu H, Doig GS, Heighes PT, Allingstrup MJ. Early enteral nutrition reduces mortality and improves other key outcomes in patients with major burn injury: a meta-analysis of randomized controlled trials. *Crit Care Med* 2018;**46**:2036–42.
49. Reintam Blaser A, Starkopf J, Alhazzani W, Berger MM, Casaer MP, Deane AM, et al. Early enteral nutrition in critically ill patients: ESICM clinical practice guidelines. *Intensive Care Med* 2017;**43**:380–98.
50. McClave SA, DiBaise JK, Mullin GE, Martindale RG. ACG clinical guideline: nutrition therapy in the adult hospitalized patient. *Am J Gastroenterol* 2016;**111**:315–34 [quiz 35].
51. Hamidzadeh K, Christensen SM, Dalby E, Chandrasekaran P, Mosser DM. Macrophages and the recovery from acute and chronic inflammation. *Annu Rev Physiol* 2017;**79**:567–92.
52. Huang X, Venet F, Wang YL, Lepape A, Yuan Z, Chen Y, et al. PD-1 expression by macrophages plays a pathologic role in altering microbial clearance and the innate inflammatory response to sepsis. *Proc Natl Acad Sci U S A* 2009;**106**:6303–8.
53. Traeger T, Mikulcak M, Eipel C, Abshagen K, Diedrich S, Heidecke CD, et al. Kupffer cell depletion reduces hepatic inflammation and apoptosis but decreases survival in abdominal sepsis. *Eur J Gastroenterol Hepatol* 2010;**22**:1039–49.
54. Chen R, Zhang S, Liu F, Xia L, Wang C, Sandoghchian Shotorbani S, et al. Renewal of embryonic and neonatal-derived cardiac-resident macrophages in response to environmental cues abrogated their potential to promote cardiomyocyte proliferation via Jagged-1-Notch1. *Acta Pharm Sin B* 2023;**13**:128–41.
55. Harwani SC. Macrophages under pressure: the role of macrophage polarization in hypertension. *Transl Res* 2018;**191**:45–63.
56. Mouton AJ, Li X, Hall ME, Hall JE. Obesity, hypertension, and cardiac dysfunction: novel roles of immunometabolism in macrophage activation and inflammation. *Circ Res* 2020;**126**:789–806.
57. Tavener SA, Long EM, Robbins SM, McRae KM, Van Remmen H, Kubes P. Immune cell Toll-like receptor 4 is required for cardiac myocyte impairment during endotoxemia. *Circ Res* 2004;**95**:700–7.
58. Ann SJ, Chung JH, Park BH, Kim SH, Jang J, Park S, et al. PPARalpha agonists inhibit inflammatory activation of macrophages through upregulation of beta-defensin 1. *Atherosclerosis* 2015;**240**:389–97.
59. Schaefer MB, Pose A, Ott J, Hecker M, Behnk A, Schulz R, et al. Peroxisome proliferator-activated receptor-alpha reduces

- inflammation and vascular leakage in a murine model of acute lung injury. *Eur Respir J* 2008;**32**:1344–53.
60. Schmiedel BJ, Singh D, Madrigal A, Valdovino-Gonzalez AG, White BM, Zapardiel-Gonzalo J, et al. Impact of genetic polymorphisms on human immune cell gene expression. *Cell* 2018;**175**:1701–1715.e16.
 61. He S, Wang LH, Liu Y, Li YQ, Chen HT, Xu JH, et al. Single-cell transcriptome profiling of an adult human cell atlas of 15 major organs. *Genome Biol* 2020;**21**:294.
 62. Engevik AC, Kaji I, Goldenring JR. The physiology of the gastric parietal cell. *Physiol Rev* 2020;**100**:573–602.
 63. Peterson WL. The role of acid in upper gastrointestinal haemorrhage due to ulcer and stress-related mucosal damage. *Aliment Pharmacol Ther* 1995;**9**(Suppl 1):43–6.
 64. Ye Z, Reintam Blaser A, Lytvyn L, Wang Y, Guyatt GH, Mikita JS, et al. Gastrointestinal bleeding prophylaxis for critically ill patients: a clinical practice guideline. *BMJ* 2020;**368**:l6722.